STUDYING AMORPHOUS-CRYSTALLINE TRANSITIONS IN POWDERS CAUSED BY BALL-MILLING

K. Tomolya[1], D. Janovszky[2], A. Sycheva[3], A. Roósz[4]
[1]Ph.D. Research fellow, [2]Ph.D. Senior research fellow, [3]Ph.D. Research fellow, [4]Doctor of Sciences, Professor
[1,2,3,4]MTA-ME Materials science Research Group, Miskolc-Egyetemváros H-3515, Hungary

ABSTRACT

The microstructure evolution during mechanical milling was studied in $(Cu_{49}Zr_{45}Al_6)_{100-x-y}Ni_xTi_y$ (x = 0, 10; y = 0; 10) alloys. Homogenous, crystalline ingots were milled for 25 hours and amorphous or amorphous/crystalline powders were synthesized. The amorphous transformation depends on the composition of the alloys. In the case of $Cu_{49}Zr_{45}Al_6$, 15 h of milling is sufficient to reach the full amorphization measured by XRD, which is enhanced by Ti and Ti-Ni alloying elements.

INTRODUCTION

Bulk metallic glasses (BMG) have been attracted high attention in the last decades because of their unique mechanical, chemical and magnetic properties [1, 2, 3]. Cu-based and particularly Cu-Zr-Al alloys have received significant attention due to high glass forming ability, relatively high plasticity and low cost [1]. The amorphous state can be indicated by liquid and solid state techniques. Due to mechanical impacts, the crystalline structure transforms into amorphous state resulting in a fully amorphous structure or amorphous matrix composites containing fine crystals of nanometer scale. During milling, the effect of the transmitted energy causes the formation of amorphous structure in the powders. In a planetary ball-mill, both the vials and the support disk rotate around their own axes. Due to the centrifugal force produced by these rotations, the grinding balls impact to each other and to the wall of the vial, while some amount of powder is trapped in between them. Coalescence and fragmentation of the particles keep balance, because of the high mechanical stress effects caused by the balls. Repeated mechanical mixing, cold welding and fracturing take place and cause the formation of a fine powder with a changed structure [4]. These powders will be processed by powder metallurgy (PM) in order to produce BMGs. It is worth mentioning that the particle parameters define the quality of the samples produced by further technology, but this topic is not part of this manuscript.
Accordingly, in this work crystalline $(Cu_{49}Zr_{45}Al_6)_{100-x-y}Ni_xTi_y$ (x = 0, 10; y = 0; 10) alloys were ball-milled. We have monitored the microstructure evolution during mechanical milling. The milling time required to obtain a fully amorphous structure was determined as function of alloying elements.

EXPERIMENTAL

Master alloy ingots with the compositions of $(Cu_{49}Zr_{45}Al_6)_{100-x-y}Ni_xTi_y$ (x = 0, 10; y = 0; 10) were prepared by arc melting the mixtures of Cu, Zr, Al pure metals under purified argon atmosphere. Table 1 summarizes the compositions of the master alloys.

Table 1
Compositions of the master alloys

	Elements, at%				
	Cu	**Zr**	**Al**	**Ti**	**Ni**
Alloy 1	49	45	6	0	0
Alloy 2	44.1	40.5	5.4	10	0
Alloy 3	39.2	36	4.8	10	10

The master alloys were grinded and fractioned to a particle size below 300 μm for ball-milling. The mechanical milling was performed in a Pulverisette 5 high-energy ball-mill in argon atmosphere using stainless steel vial and balls with a diameter of 5, 7 and 10 mm [5]. The overall process lasted 25 h. The milling process was interrupted every hour. Each interruption was followed by a period of 2 hours to cool down the vials. The milled powder samples were extracted every 5 hours in order to examine the progress of amorphization reaction.
In order to reveal the microstructure, both the master alloys and the powders were embedded in acrylic resin, then polished and etched with 0.5 % hydrofluoric acid for 5 sec. The structure of each master alloy ingot and each powder was investigated by a Hitachi S4800 Field Emission Scanning Electron Microscope (SEM) equipped with a Bruker AXS Energy-dispersive X-ray Spectrometer (EDAX) system, and a Philips PW 1830 X-ray diffractometer (XRD) with monochromatized CuKα radiation of 0.15418 nm wavelength using an anode voltage of 40 kV and a current of 305 mA. The amorphous fraction was determined by evaluation of XRD patterns. Using a combination of free software Fityk 0.98 and software developed by us (GerKiDo), different curves can be fitted to selected measuring points. The amorphous fraction can be calculated after measuring the area under the curves described in detail in Ref. 6.

RESULTS

ANALYSIS OF THE MASTER ALLOY INGOTS

The master alloy prepared by arc melting has a high cooling rate. The surface of the sample that was in contact with the Ar atmosphere during arc melting cooled at a minimum rate of 100 K/s. The cooling rate of the bottom surface of the samples that was in contact with the inner surface of the copper crucible was considerably higher. Fig. 1 shows the XRD pattern of the master alloys with sharp peaks characterizing the crystalline structure. Some phases cannot be identified by XRD

because of the small number of constituents and unknown, metastable phases of this system. In Fig. 1a diffraction pattern of Alloy 1 is shown, which contains $AlCu_2Zr$, CuZr and an unknown phase. Fig. 1b and Fig. 1c show the diffractograms of Alloy 2 and Alloy 3.

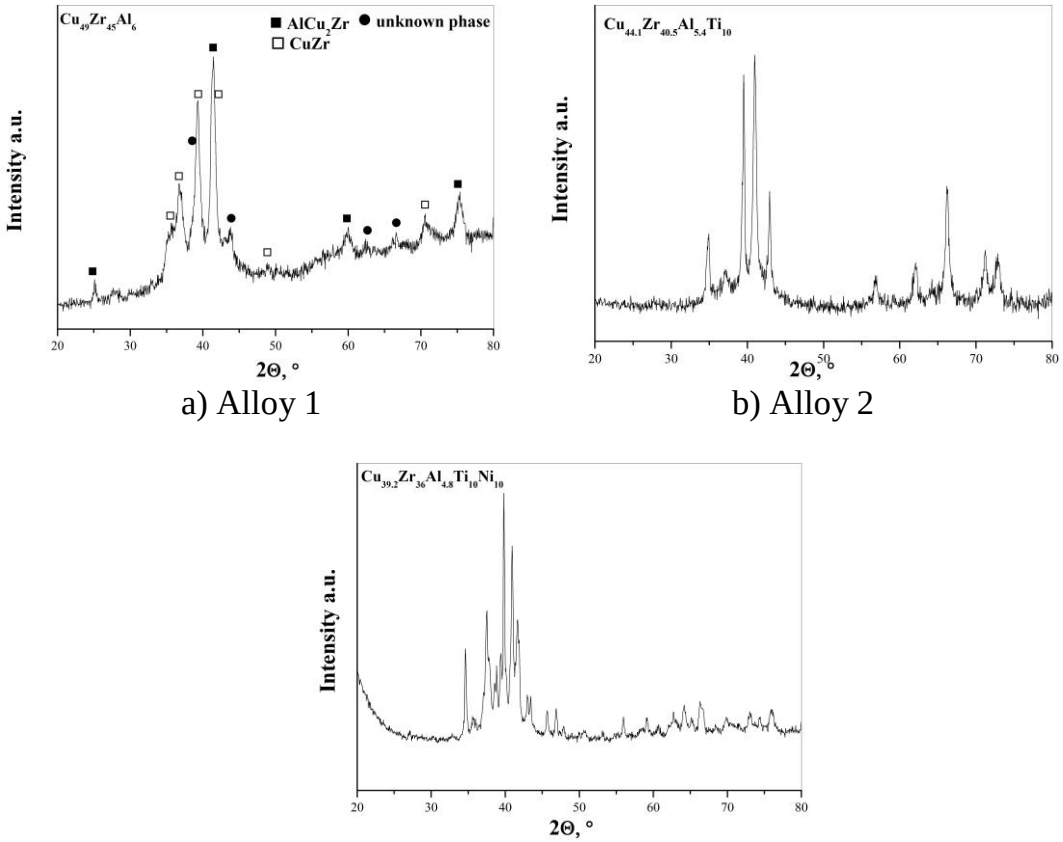

a) Alloy 1 b) Alloy 2

c) Alloy 3

Fig. 1
XRD patterns of the master alloy ingots

The microstructure of the master alloys was investigated by SEM, which is presented in Fig. 2. Phases of Alloy 1 were identified based on the microstructure observations and the XRD analysis. CuZr and an unknown phase are embedded in the fine eutectic microstructure, which constitute CuZr and $AlCu_2Zr$ phases. These phases were identified by TEM and it is published in our previous work [7]. Alloy 2 has a fine eutectic structure permeated by dendrites (phase 3). The grey phase of eutectic (point 2) is a Ti-rich phase containing all the four elements based on the EDAX analysis.

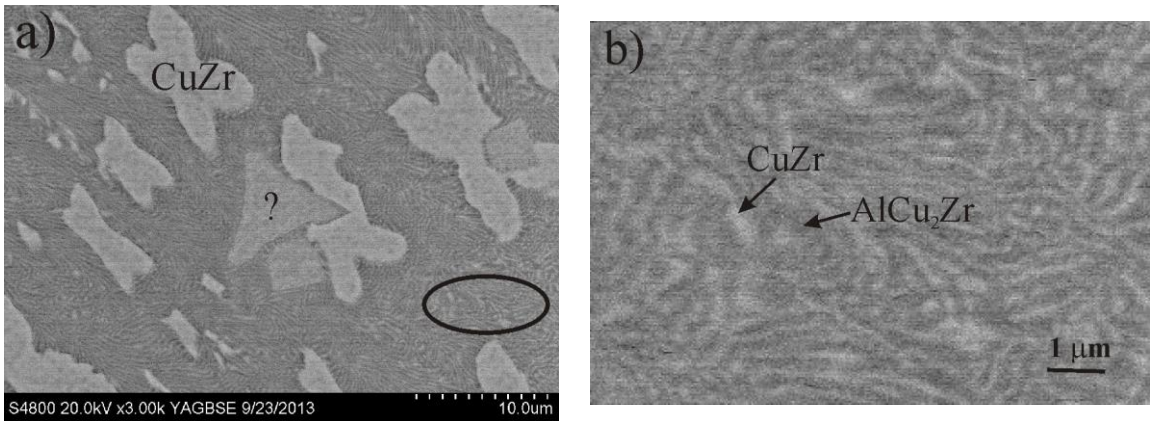

a) and b) Cross sections of Alloy 1

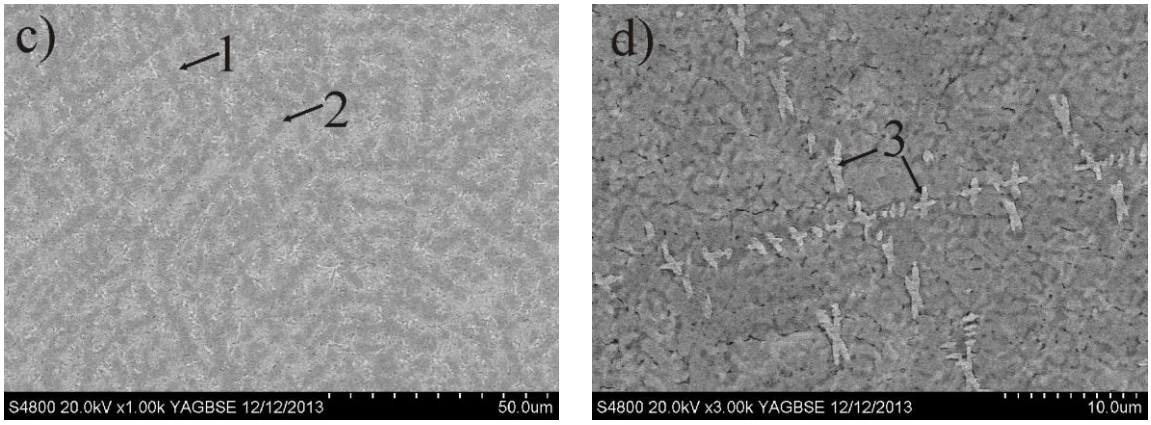

b) and c) Cross sections of Alloy 2

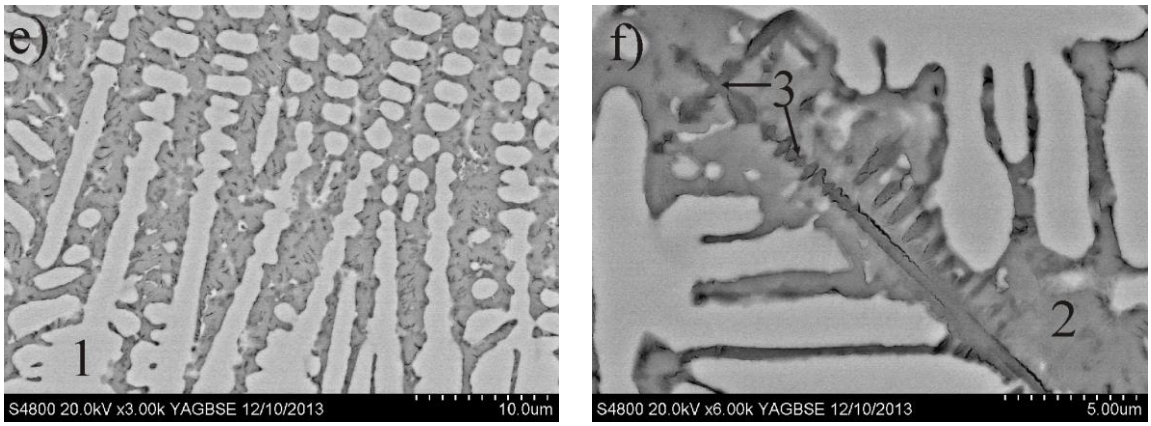

d) and e) Cross sections of Alloy 3

Fig. 2
Microstructure of the master alloy ingots

Table 2 summarizes the composition of the phases in Alloy 2 and Alloy 3 measured by EDAX. In Alloy 3, there are two dendritic phases (Fig. 2 d-e), point 1 and point 3, in the grey matrix (point 2), which dissolved more Ti. It can be seen in the case of three alloys that the structure is homogenous, which is an important attribute in the production.

Table 2
Composition of the phases in the alloys measured by EDAX

Sample	Phase	Figure	Composition, at%				
			Cu	Zr	Al	Ti	Ni
Alloy 2	1	Fig. 2 b)	51	41	2	6	-
	2	Fig. 2 b)	46	35	5	14	-
	3	Fig. 2 c)	40	45	6	9	-
Alloy 3	1	Fig. 2 d)	40	38	3	10	9
	2	Fig. 2 e)	42	30	5	15	8
	3	Fig. 2 e)	46	32	3	11	8

ANALYSIS OF THE MILLED POWDERS

Fig. 3 shows the XRD patterns of the as-milled powders, which present the phase evolution of powders occurred during ball-milling as function of the milling time.

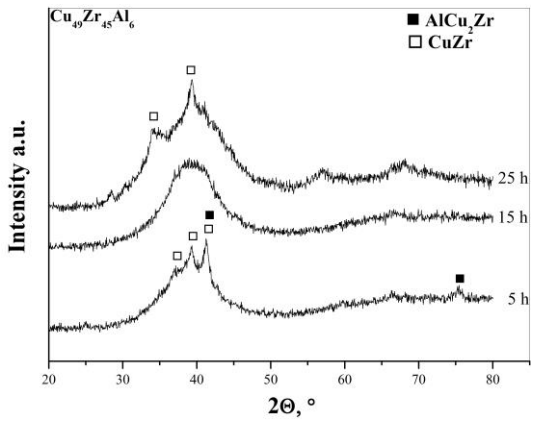

a) Alloy 1

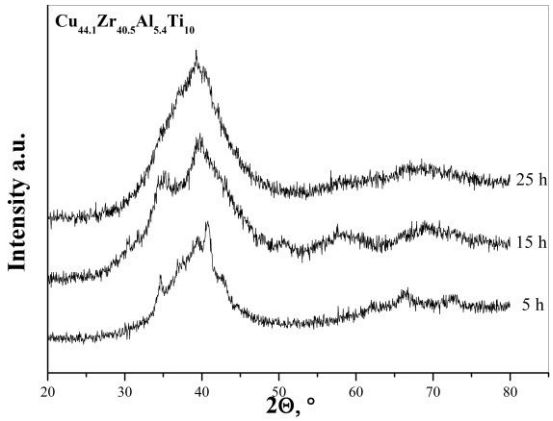

b) Alloy 2

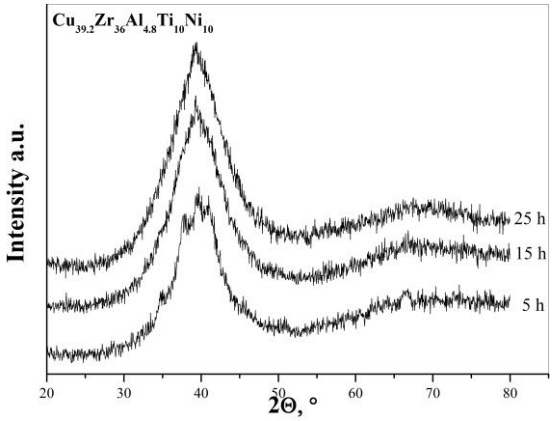

c) Alloy 3

Fig. 3
XRD patterns of the as-milled powders

The XRD pattern of crystalline alloys shows peaks belonging to the phases. During amorphization, the number and the intensity of these peaks reduce and amorphous halo appears. In the case of full amorphization only the amorphous halo remains indicating the structure. The amorphization process by ball-milling has a reversible behavior, after further milling new peaks appear, because new crystals are formed.
For all the samples studied in this work, 25 hours were selected as maximal milling time based on the results of our previous research. The diffraction peaks attributed to the crystalline phases considerably reduce with increasing milling time, but the amorphous transformation depends on the composition of the alloys.

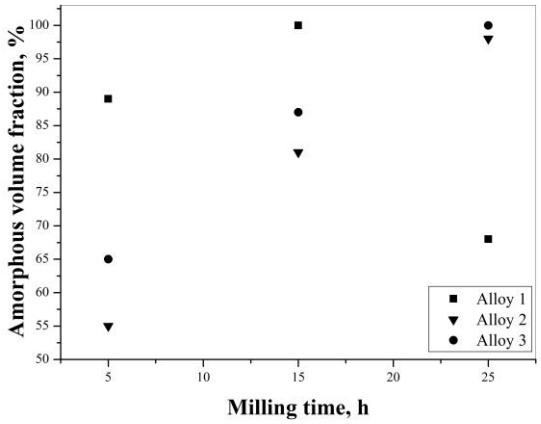

Fig. 4
Amorphous volume fraction vs. milling time

Fig. 4 represents the amorphous volume fraction in the function of milling time calculated from the XRD patterns. In the case of Alloy 1, after 5 h of milling, 85 Volume% of the structure transformed into amorphous state and after 15 h of milling the peaks disappeared and only a broad diffuse halo remained indicating full amorphization. Alloy 3 needs more time to reach the fully amorphous structure, while no complete amorphization occurs in the case of Alloy 2; it has 98 Volume% of amorphous fraction.
Table 3 summarizes the back scattered SEM images of the powders milled for 15 h and 25 h. The average particle size is 10-40 μm after 25 h of milling. In the images of polished samples after 15 h of milling, cavities and pores can be clearly seen in the particles because coagulation and fragmentation are achieved during milling and there are a lot of cracks in the particles owing to the mechanical stress. During further milling, the original phase boundaries disappeared and the phases were undistinguishable at the end of milling. Alloy 2 behaves differently from the other compositions. Cold welding of the fragmented particles does not dominate the process and the mixing of initial phases can be observed. In the images of etched samples, it can be observed that the structure of the milled powders is a mixture of the initial phases at an early stage of milling, which is no more visible after 25 h of milling even in higher resolution (Alloy 3, 25 h, etched).

Table 3
Cross section of the as-milled powders after polishing and etching

	Milling time	Polished	Etched in 0.5 % HF
Alloy 1	15 h		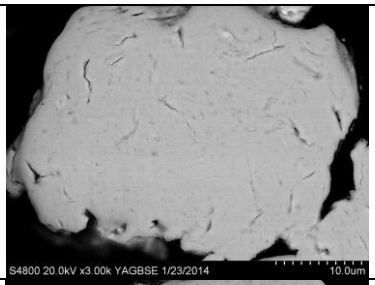
	25 h		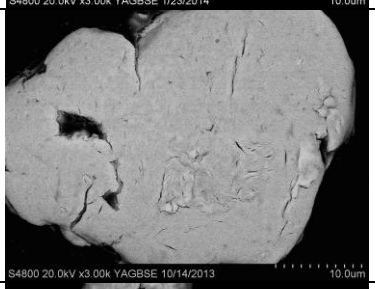
Alloy 2	15 h	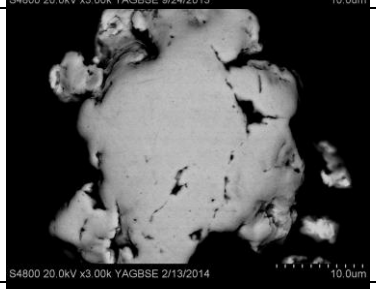	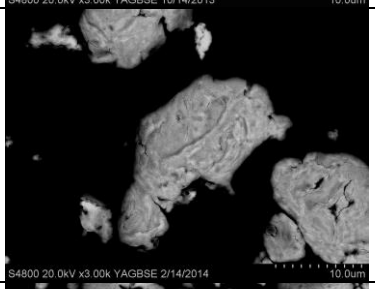
	25 h	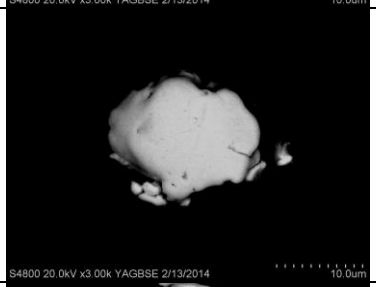	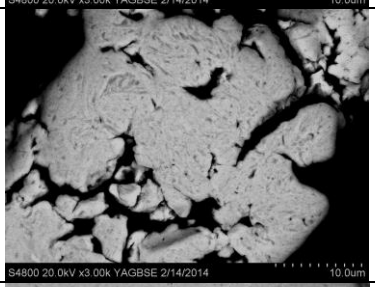
Alloy 3	15 h	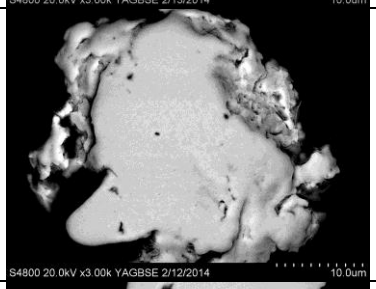	
	25 h		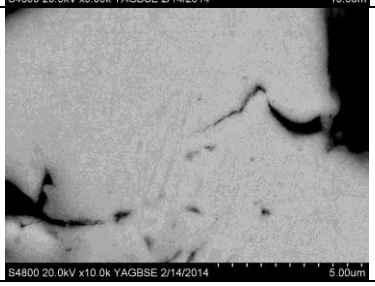

SUMMARY

In this work crystalline $(Cu_{49}Zr_{45}Al_6)_{100-x-y}Ni_xTi_y$ (x = 0, 10; y = 0; 10) alloys were ball-milled. Homogenous master alloy ingots were exposed to milling. The structure of $Cu_{49}Zr_{45}Al_6$ (Alloy 1) changes by the addition of Ti and Ti-Ni alloying elements. The diffraction peaks attributed to the crystalline phases considerably reduce with increasing milling time, but the amorphous transformation depends on the composition of the alloys, namely the phases present in the alloy. In the case of Alloy 1, 15 h of milling is sufficient to reach full amorphization measured by XRD. The Ti and Ni addition changes the milling time required for complete amorphization, because Alloy 3 needs more time to reach the fully amorphous structure, while no complete amorphization occurs in the case of only Ti alloying (Alloy 2); it has 98 Volume% of amorphous fraction.

ACKNOWLEDGEMENT

This work has been carried out as part of the TÁMOP 4.2.4.A/2-11-1-2012-0001 project within the framework of the New Hungarian Development Plan. The realization of this project is supported by the European Union, co-financed by the European Social Fund.

REFERENCES

[1] M. Abbasi, R. Gholamipour, F. Shahri: **Glass forming ability and mechanical properties of Nb-containing Cu−Zr−Al based bulk metallic glasses.** Trans. Nonferrous Met. Soc. China 23(2013) 2037−2041

[2] S. Pauly, J. Das, J. Bednarcik, N. Mattern, K.B. Kim, D.H. Kim, J. Eckert: **Deformation-induced martensitic transformation in Cu–Zr–(Al,Ti) bulk metallic glass composites.** Scripta Materialia 60 (2009) 431–434

[3] Y. Wu, H. Wang, H.H. Wu, Z.Y. Zhang, X.D. Hui, G.L. Chen, D. Ma, X.L. Wang, Z.P. Lu: **Formation of Cu–Zr–Al bulk metallic glass composites with improved tensile properties.** Acta Materialia 59 (2011) 2928–2936

[4] K. Tomolya, D. Janovszky, M. Benke, A. Sycheva, M. Sveda, T. Ferenczi, P. Pekker, I. Cora, A. Roósz: **Microstructure evolution in CuZrAl alloys during ball-milling.** Journal of Non-Crystalline Solids 382 (2013) 105–111

[5] K. Tomolya, D. Janovszky, T. Janvari, A. Sycheva, F. Tranta, J. Solyom, T. Ferenczi, A. Roosz: **Consolidation of Cu58Zr42 amorphous/nanocrystalline powders by PM.** J. Alloys Compd. 536 (2012) S154-S158

[6] G. Körösy, K. Tomolya, D. Janovszky, J. Sólyom: **Evaluation of XRD analysis of amorphous alloys.** Mater. Sci. Forum 729 (2013) 419-423

[7] K. Tomolya, D. Janovszky, A. Sycheva: **Amorphization of CuZr based alloy powders by mechanical milling.** Mater. Sci. Forum, article in press (2014)